Acknowledgements The research presented here is supported by the National Natural Science Foundation of China (52078317), Natural Science Foundation of Jiangsu Province for Excellent Young Scholars (BK20211597), project from Bureau of Housing and Urban-Rural Development of Suzhou (2021-25; 2021ZD02; 2021ZD30), Bureau of Geology and Mineral Exploration of Jiangsu (2021KY06), China Tiesiju Civil Engineering Group (2021-19), CCCC First Highway Engineering Group Company Limited (KJYF-2021-B-19), and CCCC Tunnel Engineering Company Limited (8gs-2021-04).

References

1. Wang, Q., Li, H., Xia, S., Yang, J., Zhang, W., Liao, G.Z., Wang, D.H.: Geometry of the Quaternary strata along the middle segment of the Longmen Shan and its formation mechanism: Insights from AMT, ERT and borehole data (2022)
2. Wang, L., Li, G., Liu, J., Mei, X., Zhang, Y.: Astronomical dating of quaternary strata in the south yellow sea and its indication for paleoclimatic evolution. Marine Geol, 106557 (2021)
3. Sizov, O., Volvakh, A., Molodkov, A., Vishnevskiy, A., Abakumov, E.: Lithological and geomorphological indicators of glacial genesis in the upper quaternary strata, nadym river basin, western siberia. Solid Earth **11**, 2047–2074 (2020)
4. Yu, X.H., Shen, J., Dai, X.Y., Wang, C.S.: Growth strata reveal the quaternary tectonic feature of gudian fault in songyuan, songliao basin, china. Dizhen Dizhi **40**(6), 1240–1253 (2018)
5. Deng, C.L., Hao, Q.Z., Guo Z.T., Zhu R.: Quaternary integrative stratigraphy and timescale of china. Sci. China (2019)
6. He, X.C., Xu, Y.S., Shen, S.L., Zhou, A.N.: Geological environment problems during metro shield tunnelling in Shenzhen, China. Arabian J. Geosci., **13**(2) (2020)
7. Ren, D.J., Shen, S.L., Cheng, W.C., Zhang, N., Wang, Z.F.: Geological formation and geo-hazards during subway construction in guangzhou. Environmental Earth Sci. **75**(11), 934 (2016)
8. Fang, G., Jiang, G., Yuan, D., Polk, J.S.: Evolution of major environmental geological problems in karst areas of southwestern china. Environ. Earth Sci. **69**(7), 2427–2435 (2013)
9. Cui, Q.L., Shen, S.L., Xu, Y.S., Wu, H.N., Yin, Z.Y.: Mitigation of geohazards during deep excavations in karst regions with caverns: a case study. Eng. Geol. **195**, 16–27 (2015)
10. Yoo, C., Kim, S.B.: Three-dimensional numerical investigations of new Austrian tunnelling method (NATM) twin tunnel interactions. Can. Geotech. J. **45**(10), 1467–1486 (2008)
11. Yilmaz, I.: GIS based susceptibility mapping of karst depression in gypsum: a case study from Sivas basin (Turkey). Eng. Geol. **90**(1–2), 89–103 (2007)
12. Editorial Department of China Journal of Highway and Transport. Review of Academic Research on Subgrade Engineering in China ·2021. China J. Highway Transport, **34**(3), 49 (2021) (in Chinese)
13. Ye, G.L., Hashimoto, T., Shen, S.L., Zhu, H.H., Bai, T.H.: Lessons learnt from unusual ground settlement during Double-O-Tube tunneling in soft ground. Tunn. Undergr. Space Technol. **49**, 79–91 (2015)
14. Ni, J.C., Cheng, W.C.: Characterising the failure pattern of a station box of Taipei rapid transit system (TRTS) and its rehabilitation. Tunn. Undergr. Space Technol. **32**, 260–272 (2012)
15. Shen, S.L., Wu, H.N., Cui, Y.J., Yin, Z.Y.: Long-term settlement behavior of the metro tunnel in Shanghai. Tunn. Undergr. Space Technol. **40**, 309–323 (2014)
16. Gong, Q.M., Yin, L.J., She, Q.R.: TBM tunneling in marble rock masses with high in situ stress and large groundwater inflow: a case study in China. Bull. Eng. Geol. Environ. **72**(2), 163–172 (2013)
17. Zhao, K., Janutolo, M., Barla, G., Chen, G.X.: 3D simulation of TBM excavation in brittle rock associated with fault zones: the Brenner Exploratory Tunnel case. Eng. Geol. **181**, 93–111 (2014)

18. Xu, Y.S., Shen, S.L., Ma, L., Sun, W.J., Yin, Z.Y.: Evaluation of the blocking effect of retaining walls on groundwater seepage in aquifers with different insertion depths. Eng. Geol. **183**, 254–264 (2014)
19. Ji, F., Lu, J.F., Shi, Y.C., Zhou, C.H.: Mechanical response of surrounding rock of tunnels constructed with the TBM and drillblasting method. Nat. Hazards **66**(2), 545–556 (2013)
20. Lai, K., Ren, Y.S., Hao, Y.J., Sun, Q., Liu, J., Jun-Ying, L.I.: Formation age and geological significance of yangbishan bif type iron deposit in jiamusi area, heilongjiang. Global Geol. (2017)
21. Zhu, W.: Geological and geochemical characteristic analyses of lower cambrian hetang formation in jiangshan-tonglu area. Acta Geologica Sinica (English edition) **93**(z2) (2019)
22. Wang, J., Wu, Y., Liu, X., Yang, T., Wang, H.: Zhu, Y,: Areal subsidence under pumping well–curtain interaction in subway foundation pit dewatering: conceptual model and numerical simulations. Environmental Earth Sci. **75**(3), 198 (2016)
23. Zhang, H.Z., Ya-Nan, L.I.: University L N . Research on the influence of the recharge of deep foundation pit dewatering to the surface subsidence. J. Langfang Normal University (Natural Science Edition) (2019)
24. Li, X., Zhou, T., Wang, Y., Han, J., Wen, J.: Response analysis of deep foundation excavation and dewatering on surface settlements. Adv. Civil Eng. **2020**(6), 1–10 (2020)
25. Zhaolin, M. A., Wang, X., Jiao, L., Survey.: Analysis of influence of dewatering of deep foundation pit on ground surface settlement. Low Temperature Architect. Technol. (2017)
26. Liu, J., Huo, J.: Analysis of influence of well point dewatering on surrounding environment in deep foundation excavation. Const. Technol. (2019)
27. Ahmed, M.D., Shiekha, A.A., Al-Obaidy, B.: Damage pattern scope prediction of well point dewatering on building foundation. In: 2nd International Conference on Engineering Sciences, at the University of Karbala-College of Engineering (2018)
28. Ahmed, M.D., Khudair, B.H., Shiekha, A.A.: Damage pattern scope prediction for well point dewatering on building foundations. Iop Conference, 433 (2018)
29. Xue, B.J.: On drainage and dewatering measures in construction of architectural projects. Shanxi Architecture (2013)
30. Zeng, C.F., Zheng, G., Zhou, X.F., Xue, X.L., Zhou, H.Z.: Behaviours of wall and soil during pre-excavation dewatering under different foundation pit widths. Comp. Geotech., **115**(Nov), 103169.1-103169.13 (2019)
31. Wang, Z.: Numerical analysis of deformation control of deep foundation pit in Ulanqab city. Geotech. Geol. Eng., 1–13 (2021)
32. Haibo, L.I.: Selection of deep foundation excavation support and dewatering style. Construction Technol. (2017)

Roof Condition Characteristics Affecting the Stability of Coal Pillars and Retained Roadway

Quang Phuc Le and Van Chi Dao

Abstract The stability of the retained roadway next to the coal pillar in the longwall mining system is mainly affected by displacement and rock pressure of the roof rock layers of the coal seam. With the objective of forecasting negative impacts in underground coal mining, this article analyzes the roof structure of the coal seam to illustrate the mechanism that causes instability of roadway retained in different roof conditions. A computer program is then used to simulate and assess the instability of the coal pillars and roadways in various roof variations according to the geological and technical conditions of the Khe Cham mine #11 seam. The results show that lowering and rotation of the console of main roof seriously affect the stability of the protective coal pillars. Vertical stresses distribution on the coal pillar increases significantly when the thickness of the immediate roof rock is very thin and insufficient to fill the goaf. Therefore, corresponding to different roof conditions, there is an effective solution for coal pillar design and roadway support to ensure production safety. This article can be used as a reference to designate technical recommendations in similar geological conditions.

Keywords Mining system · Temporary coal pillars · Main roof collapse state · Numerical modeling · Hard-caving main roof rocks · Deformation of the roadways · Roadway retained

1 Introduction

Controlling roadway deformation, increasing coal recovery rate, and reducing production costs have always been important strategic goals of underground coal mines [1, 2]. In underground coal mines of Vietnam, the longwall mining system

Q. P. Le (✉) · V. C. Dao
Hanoi University of Mining and Geology, 18 Vien Street, Hanoi 100000, Vietnam
e-mail: lequangphuc@humg.edu.vn

V. C. Dao
e-mail: daovanchi@humg.edu.vn

L. Q. Nguyen et al. (eds.), *Advances in Geospatial Technology in Mining and Earth Sciences*, Environmental Science and Engineering,
https://doi.org/10.1007/978-3-031-20463-0_29

with the retention of coal pillars to protect the roadway (Fig. 1) has long been chosen for wide use because of its advantages, such as (1) coal pillar has the role of isolating goaf with the retained roadway for the adjacent panel, (2) a high level of production concentration and ability to raise output from longwall face. However, its significant disadvantages are the loss of coal in the coal pillars accounting for 20% of the reserve and the high danger of rock bump in the high roof pressure area. In addition, when the width of the coal pillar is not properly designed, it will lead to the risk of roadway deformation problems, and the maintenance and repair costs are high.

Calculating the design of coal pillars and roadway supports is a complex process, as it considers a combination of factors of geology, engineering, and experience. The fact shows that abutment pressure is the main cause of instability of coal pillars and roadways. As a rule, after coal is extracted from the longwall face, the roof rock will crack and collapse into the goaf. Simultaneously, the stress in the rock mass around the goaf is redistributed until the displacement of the rock layers stops [3, 4]. The characteristics of appearance, distribution, and maintenance of stress elevation, abutment pressure on the edge of the coal seam, caused by the displacement of the roof rock layers, depend on their structural characteristics. The negative effects arising from the formation of the raised pressure zone on the retained roadway and coal pillars next to the goaf are roadway deformation, destruction of coal pillars, increased roadway repair costs, increased mining works, and occupational accidents.

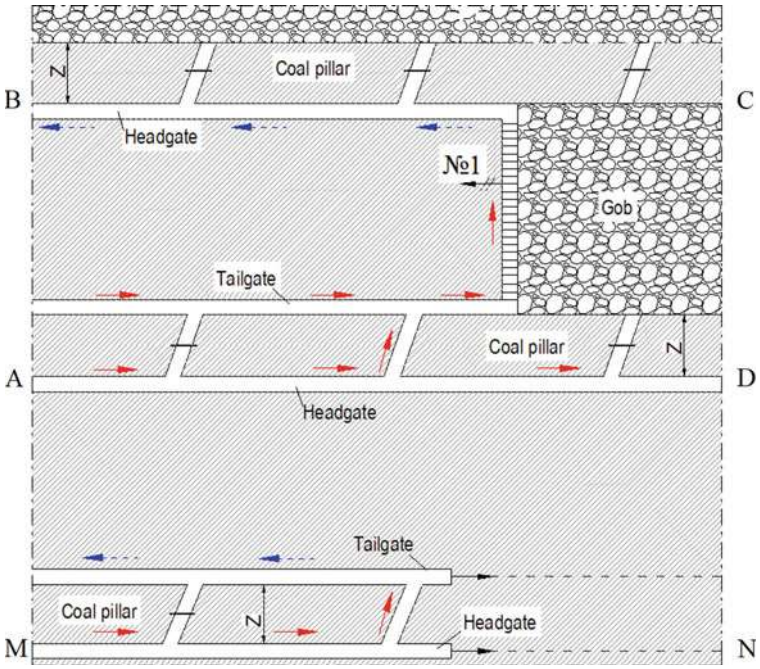

Fig. 1 Plan of longwall mining system applied in underground coal mines in Vietnam

The final state of the abutment pressure around the goaf is determined by the structural condition of the immediate roof and the main roof. As a rule, three collapse zones of roof rock [5, 6] will form above the goaf (from bottom up), which are cave zone, fractured zone, and continuous deformation zone. The value of the abutment pressure will be proportional to the size of the collapse area and depends on the properties of the roof rock layers. When the immediate roof is thick enough, the goaf can be completely backfilled by the cave rock, and the main roof will not crack. The intact main roof can then bear the load of the rock layers above and lead to safer coal seam mining because the retained roadway and coal pillars are less affected by the rock pressure. In contrast, when the main roof is cracked, the height of the roof's failure zone increases and leads to serious effects of abutment pressure caused by displacement of the roof rock layers.

Many studies on roadway stability control have been performed recently, but most of these works focus on the problem of roadway stability under a certain roof condition. For example, Feng et al. [7] studied the size and location of retained roadway under soft rock roofs. Kvardakov et al. [8] proposed a rigid and flexible support for the roadways under the hard rock roof. Zhang et al. [9–11] studied the stability of the roadway under the roof layer containing coal. Wang [12] proposed a method of constructing protective pillar from artificial materials to protect the retained roadway under complex roofs. Ning [13] analyzed the stability of the artificial pillar strip construction on the coal seam with large slope angle.

It can be seen that the study of the difference in roof rock conditions to provide solutions for designing coal pillars and supporting the roadway is absent. In addition, the high stress [14] and elastic–plastic rock mechanics [15–17] in deep mines make it more difficult to control the stability of the roadway and coal pillars. Therefore, the research problem that provides reliable data for finding solutions to design coal pillar and support roadway before impacts from unstable sources is that the roof rock layers will have great significance for the sustainable development of underground coal mining industry.

2 Research Methods

In this paper, the theoretical analysis of the roof rock structures of the coal seam and their collapse characteristics in the goaf is used. Then, a computer program is used to simulate the stability of the coal pillars and the deformation of the roadway during the mining of the panels with different cases of roof rock conditions. In our analysis, we use the typical geological conditions from the Khe Cham coal mine in the Quang Ninh coal basin, which has all the typical roof rock features of Vietnam's underground coal mines.

Building simulation models

A numerical model using the program FLAC3D [18] is developed to investigate the relationship between the stability of a reusable roadway and different conditions

of roofs in shallow coal seams. FLAC3D is a software for numerical simulation of the geotechnical state of a continuum for studies of stress–strain state of rock mass. Such an analysis is practiced in the design of structures, strength calculations, research and testing, as well as for solving inverse problems of determining the margin of safety of structures. FLAC3D uses an explicit finite volume specification that captures the complex behavior of models going through several successive stages in their state, experience large displacements and deformations, taking into account nonlinear material behavior or instability (including the possibility of failure over large areas or a general loss of continuity).

The size of the model is 310 m × 200 m × 150 m, which is determined based on a sensitivity analysis of the model with respect to the size and density of the network. Two mining panels #1 and #2 and roadways are included in the model as shown in Fig. 2. In this model, roadways have a rectangular cross-section of 4 m wide and 3.0 m high. Assuming that the coal pillar is built in the model with a width of 20 m. A vertical stress of 7.0 MPa is applied to the upper boundary of the model to simulate natural loading, and the upper specific gravity is assumed to be 0.025 MN/m^3, and gravity is also applied [19]. The horizontal offset of the four vertical planes of the model is constrained to the normal direction, and the vertical offset at the bottom of the model is set to zero. This model uses the Mohr–Coulomb model.

In this model, the immediate roof is mudstone, and the main roof is sandstone. The thickness of the main roof is set to a certain value of 19 m, and the thickness of the immediate roof is changed according to the cases with the maximum value being

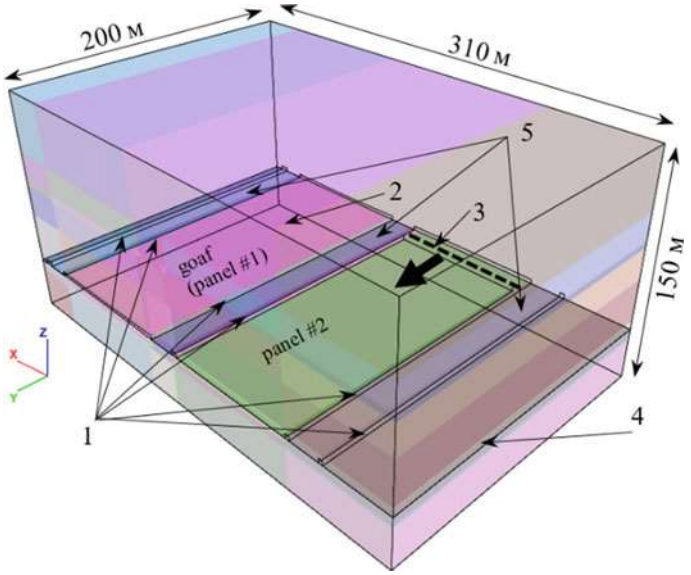

Fig. 2 Model configuration made with the program FLAC3D: 1—roadways, 2—goaf of mining panel #1, 3—mining panel #2, 4—coal seam, 5—coal pillar

able to fill the goaf when a 3-m-thick coal seam is exploited and can be calculated according to Eq. (1).

The model is built with the values of the coefficients taken as $k_p = 1.25$ and $k = 0.05$. Thus, the maximum thickness of the immediate roof determined in the corresponding model will be 12 m (when $\Delta h = 0$).

The article applies an assumption with 5 different types of roof structures to simulate and evaluate their effects on the stability of coal pillar and roadways. The parameters of the 5 types of roof structures are presented in Table 1.

In the model, the rock floor is assumed to be a siltstone with a thickness of 3 m. The rock strata consisting of sandstone, siltstone, mudstone, and coal are referred to as Mohr–Coulomb constitutive material. The mechanical parameters of the rock and coal layers used in this model are collected according to the results of testing rock samples in the laboratory and on-site statistical investigation at the Khe Cham coal mine, Vietnam. The physico-mechanical properties of the rock and coal layers are listed in Table 2.

In this simulation, the numerical model is solved using the following steps: (1) calculation of the initial stress caused by gravity; (2) driving roadways; (3) mining panel #1; and (4) mining panel #2. Five different variants (Table 1) of the roof are implemented in the model. The scheme of the algorithm for performing the simulation is shown in Fig. 3.

Table 1 Thickness of rock strata in different simulation schemes

Type roof seams	Thickness of seams (m)	Thickness of the immediate roof, h_1 (m)	Thickness of the main roof, h_2 (m)	Sink the main roof, Δh (m)
I	3,0	12	19	0
II	3,0	9	19	0.69
III	3,0	6	19	1.44
IV	3,0	3	19	2.19
V	3,0	0	19	2.94

Table 2 Physico-mechanical properties of rocks

Type rock	Tensile strength (MPa)	Bulk modulus (GPa)	Shear modulus (GPa)	Poisson's ratio	Cohesion (MPa)	Friction angle (deg.)	Density (kg/m3)
Sandstone	1.6	7.456	3.244	0,31	3,2	34	2780
Mudstone	0.9	2.333	0.955	0,32	2,1	30	2550
Siltstone	1.2	1.822	0.607	0,35	1,8	26	2250
Coal	0.4	0.748	0.484	0,26	1,5	19	1450

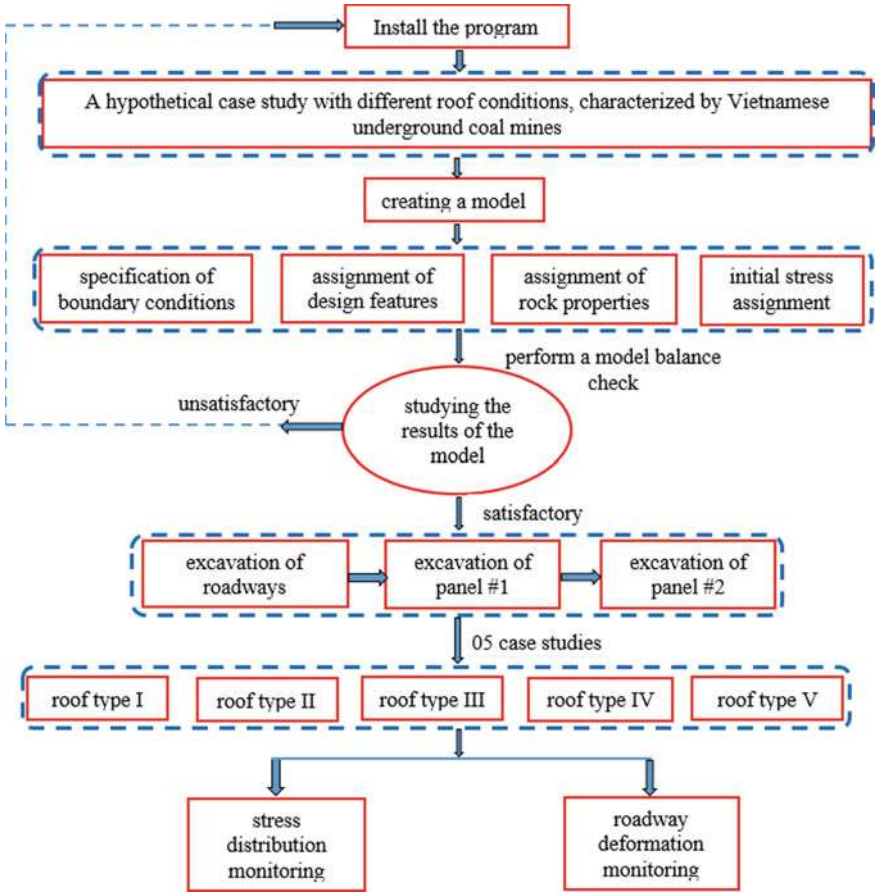

Fig. 3 Block diagram of the algorithm for performing numerical simulations with the FLAC3D program

3 Results and Discussion

3.1 Analysis of the Roof Rock Structures of the Coal Seam and Their Collapse Characteristics

The displacement of the roof rock layers above the goaf forms the console beams of the main roof on the edge of the coal pillar [20, 21]. Over time, the load of the roof rock layers above the console causes the edge of the coal pillar next to the goaf to be compressed and destroyed, facilitating the cracking and fracture process of the console. This static and dynamic load has a strong influence on the stability of the coal pillar and retained roadway [22–24]. As shown in Fig. 4, four deformation

models have been constructed to illustrate the collapse of the main roof in different roof structures of the coal seam.

Figure 4 depicts different roof conditions in the following cases.

When the thickness (h_1) of the immediate roof is very thick, it collapses and is capable of filling the goaf (Fig. 4a). In this case, the main roof has almost no cracks, and most of the load of the rock layers is supported by the intact main roof. The influence of the load of the roof rock layers on the coal pillar and the roadway is minimal.

When the immediate roof has a small thickness (h_1), it collapses but cannot fill the goaf (Fig. 4b, c). Therefore, the main roof will collapse on the edge of the coal pillar with the rotation angle φ and subsidence Δh. The displacement of the block of the main roof when fracture can be simulated as a rotation around the crack above the coal pillar. In this situation, the collapsing process of the console beam will compress the underlying rock, including the coal pillar and retained roadway. The estimated impact intensity of rock pressure on the coal pillar is larger than that in the first case.

The subsidence Δh of the main roof console on the edge of the coal pillar can be calculated:

$$\Delta h = m_s \times (1 - k) - \left(k_p - 1\right) \times h_1 \tag{1}$$

where m_s—the thickness of the coal seam m, k—the coefficient of coal loss in the goaf, k_p—the coefficient of loose expansion of caved rocks of immediate roof collapse, h_1—the thickness of the immediate roof.

The rotation angle of the console of the main roof when collapsing can be calculated by:

$$\varphi = \sin^{-1}\left(\frac{\Delta \mathrm{h}}{\mathrm{L}}\right) \tag{2}$$

where L—the length of the collapse block of the main roof.

When the coal seam lacks an immediate roof ($h_1 = 0$) (Fig. 4d), the console of the main roof is located directly on the coal seam. Therefore, the entire load of the roof layers is transmitted directly to the edge of the coal seam, where the coal pillar and roadway are designed. When the coal seam is exploited, a large space ($\Delta h = m$) appears below the console of the main roof. The large deformation energy generated by the console rotation and subsidence is directly absorbed by the coal pillar. As a result, the coal pillar is strongly compressed and weakened significantly and is the cause of rock bump incidents, deformation, and roadway collapse. In this situation, roadway support should be focused on reducing the effect of main roof displacement.

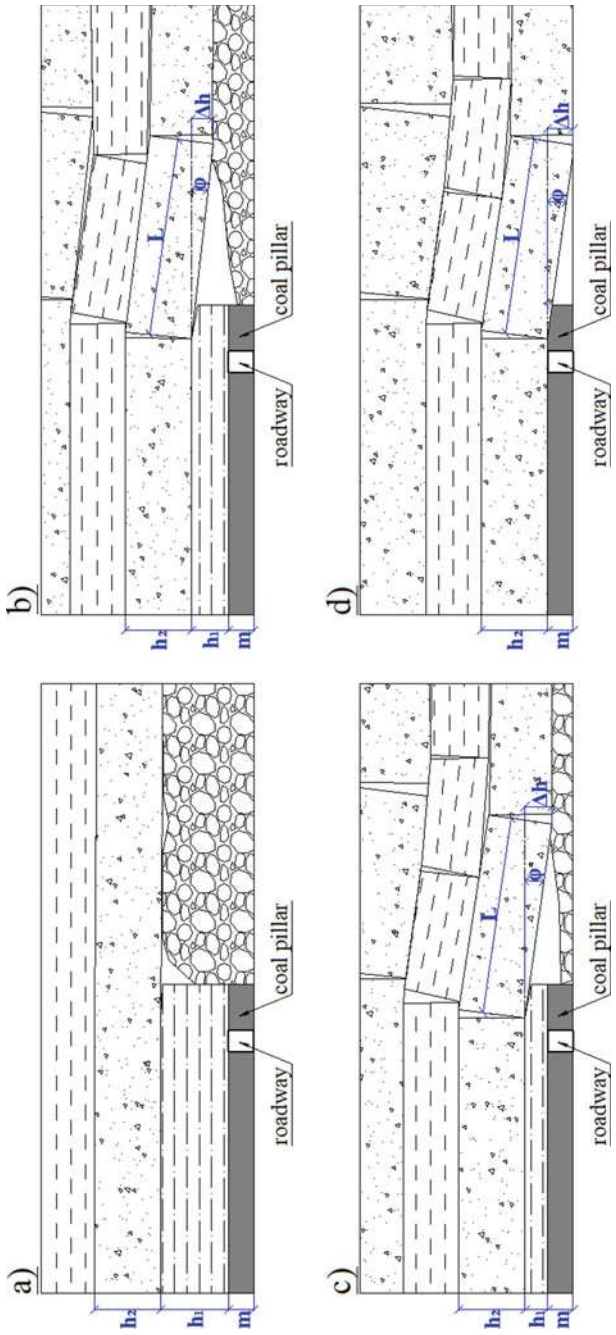

Fig. 4 Sate of collapse of the main roof in various roof structures: **a** very thick immediate roof, **b** immediate roof of medium thickness, **c** thin immediate roof, **d** no immediate roof

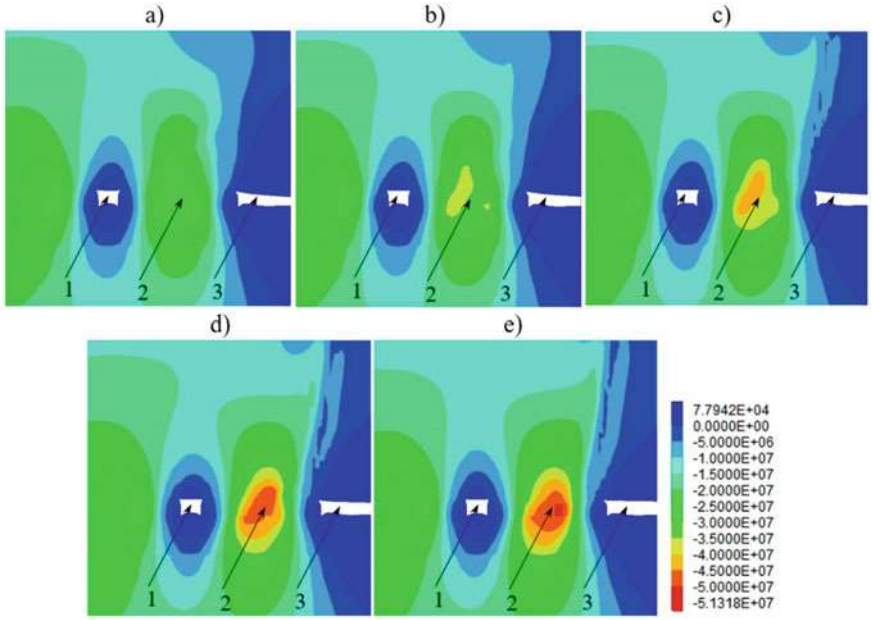

Fig. 5 Vertical stresses distribution around roadway and coal pillar (legend of vertical stress, Pa): **a** roof type I, **b** roof type II, **c** roof type III, **d** roof type IV, **e** roof type V, 1—retained roadway, 2—coal pillar, 3—goaf

3.2 Numerical Simulation Results

Results of monitoring stress evolution

The results of stress monitoring on coal pillars in different roof types are shown in Figs. 5 and 6. The position of the stress monitoring cross-section is taken at a distance of 20 m in front of longwall face #2.

Figures 5 and 6 show that there is a change in stress distribution on coal pillars when the roof rock structure changes. When the roof is very thick (types I, II), the stress distribution on the coal pillar is in the form of a double arch with two stress peaks distributed near the edges of the coal pillar. These stress peaks tend to get closer together as the immediate roof thickness decreases. The maximum value of the stress peak also increased, respectively, from 34 MPa (type I) to 39 MPa (type II). However, it is observed that, in the middle of the coal pillar in these two cases, there appears an elastic region (concave part of the stress curve) to ensure that the coal pillar always reaches a stable state.

Next, these two stress peaks merge into a single stress peak, and the integrated maximum stress on it also increases as the thickness of the immediate roof rock is further reduced. The value of stress peaks also increased from 42 MPa (type III) to 49.5 MPa (type IV) and 50.1 MPa (type V). The evolved into a single stress peak

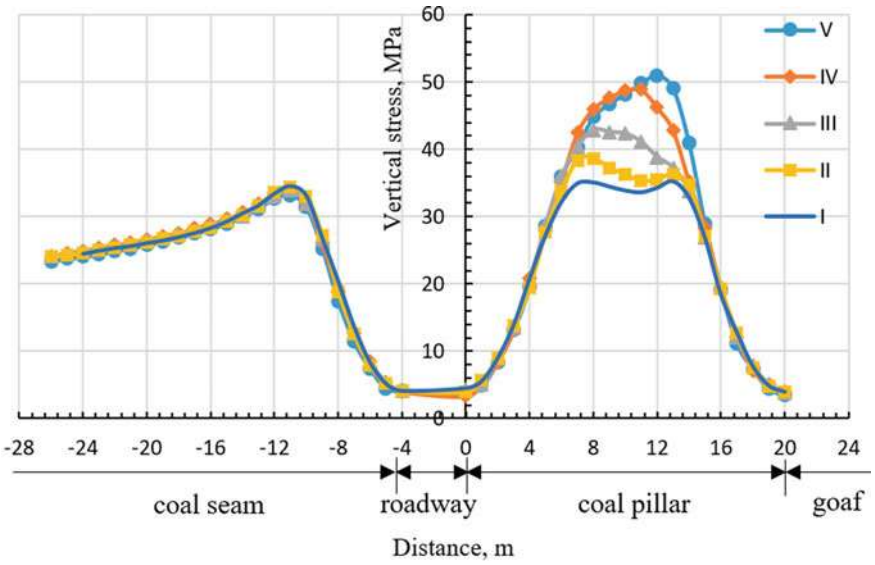

Fig. 6 Distribution of vertical stresses on coal pillar and coal seam when changing the structure of rock roof layers

demonstrated that the elastic region at the center of the coal pillar is lost and that the plastic deformation region has completely invaded it. The increase in stress also proves that when there is no immediate roof or it has a small thickness, the main roof will directly act on the coal pillar with great intensity (from the console formation of the main roof and collapse in the goaf). And so, the coal pillar will have to work in the maximum support mode to resist the pressure of the main roof, as well as the ability to protect the roadway. However, it has been shown that, when the stress on the coal pillar increases beyond the maximum limit, it will decrease suddenly due to the breaking of the cohesion of the coal mass and the formation of many cracks distributed in the coal pillar [10, 11]. Basically, the coal pillar is then damaged and causes serious deformation of the retained roadway. The simulation results show that the amplitude of stress change from type IV to type V is very small, which proves that it has reached the maximum state and will suddenly decrease after that.

Results of monitoring deformations

Figures 5 and 6 show that the coal pillar with a width of 20 m shows no signs of being destroyed, as the maximum stress peak on it is still higher than that on the coal seam. That is, the coal pillar still plays the main bearing role in all cases and eliminates the possibility of being destroyed under the pressure of the roof rock. Therefore, the roadway is maintained in a "mass-pillar" structure with a stable coal pillar, and the convergence of the roadway is assumed to be observed in this case. The evolution of the roadway convergence during the mining of longwall faces 1 and 2 is shown in Figs. 7 and 8. It is seen that the convergence of the roadway is greater when the

immediate roof is thinner. This corresponds to the result that increasing vertical stress should increase roadway convergence. The special case is that the roof convergence of the roadway will decrease when there is no immediate roof. It is explained that the immediate roof is mudstone with low strength, and the formation of the crack system in it is greater than the main roof. For example, within the distance of 100 m behind longwall face #1, the roof convergence is 19 cm (type IV) versus 14 cm (type I) (Fig. 7a). However, this is not much different when the coal pillar is assessed as showing no signs of being destroyed.

In all cases, the convergence deformation of the roadways mostly takes place in the stage when they are about 30 m in front of longwall face #1, about 80 m behind longwall face #1, and especially, they change intensely when approaching longwall face #2 (about 40 m in front of longwall face #2). The maximum convergence of the roof increases from 27 cm (type I) to 37 cm (type IV) (Fig. 8a). The maximum convergence value of the floor increases from 49 cm (type I) to 65 cm (type V) (Fig. 8d). The maximum convergence value of the right rib (coal pillar side) has increased from 49 cm (type I) to 58 cm (type V) (Fig. 8c), and that of the left rib (coal seam side) is from 17 cm (type I) to 25 cm (type V) (Fig. 8b). It should be noted that, in the roof and floor of the retained roadway, large convergence occurs near the coal pillar side, and on the ribs of the roadway, the maximum convergence occurs in its center. The deformation on the left rib (coal seam side) is always smaller than that on the right rib (coal pillar side) in all cases. It is explained that the stress distributed on the coal pillar is always higher than that on the coal seam side.

In fact, the final deformation of the surrounding rock with respect to the usable space of the roadway consists of integral motion and volume expansion in the surrounding rock mass, due to the formation of cracks and fissures. For roof layers, the contribution of volume expansion to its final deflection is greatly reduced when the roadway is directly covered by a hard main roof. In addition, the rotation and subsidence of the rock console on the main roof compress the coal pillar more than on the coal seam side (Fig. 4). As a result, the coal pillar and right rib expand in the horizontal direction and are compressed in the vertical direction. Meanwhile, a vertical force is transmitted to the floor through the coal pillar, causing large heaving of the floor.

It should be noted that, when the coal pillar loses its bearing capacity, it means that the retained roadway will be strongly deformed. In the analyzed cases, coal pillar tends to be weaker as the immediate roof thickness decreases, and the deformation of the retained roadway also increases according to this law. Therefore, additional solutions are needed to increase the stability of the coal pillar and ensure the control of retained roadway deformation.

4 Conclusion

In this paper, the stability of the coal pillar and the retained roadway under the different roof conditions have been studied. The roof structure, stress distribution,

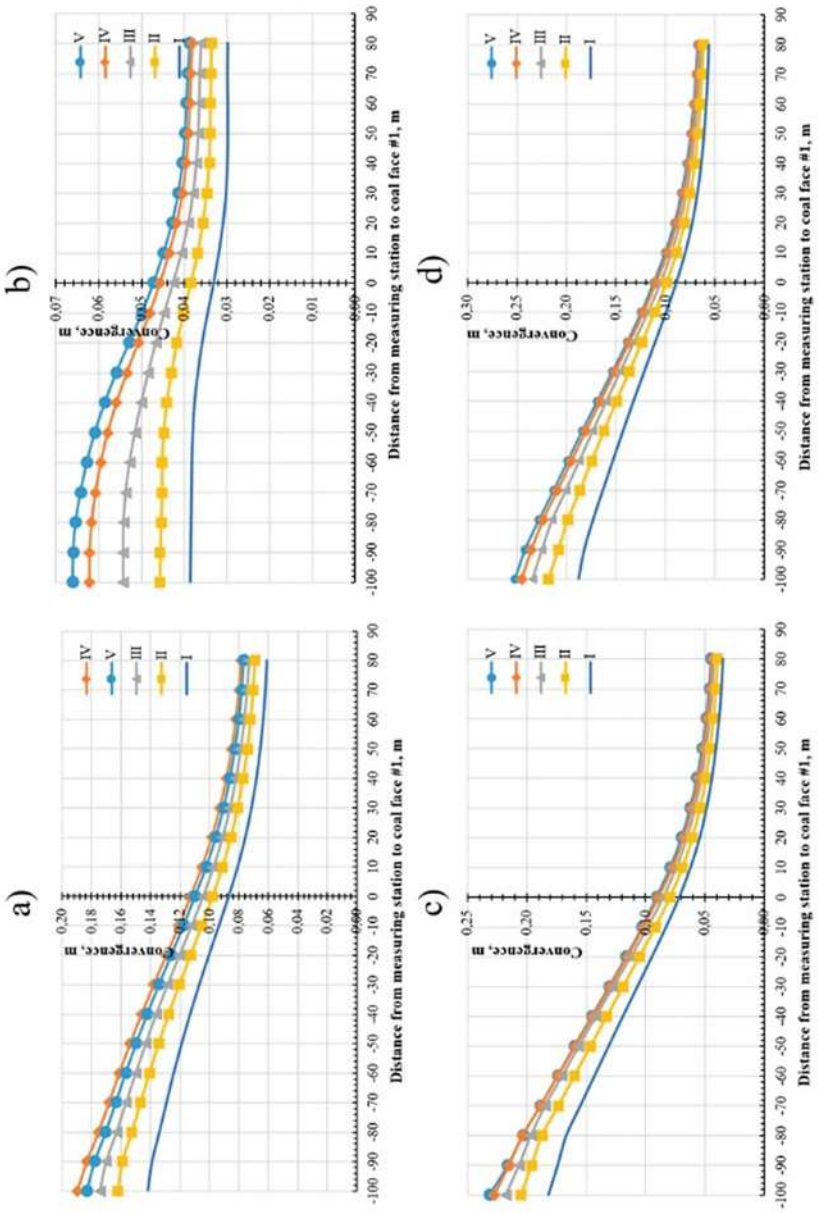

Fig. 7 Convergence of roadway before and after the coal face #1 corresponding to different roof rock structures: **a** roof subsidence, **b** convergence of the left rib (coal seam side), **c** convergence of the right rib (coal pillar side), **d** heaving of the floor

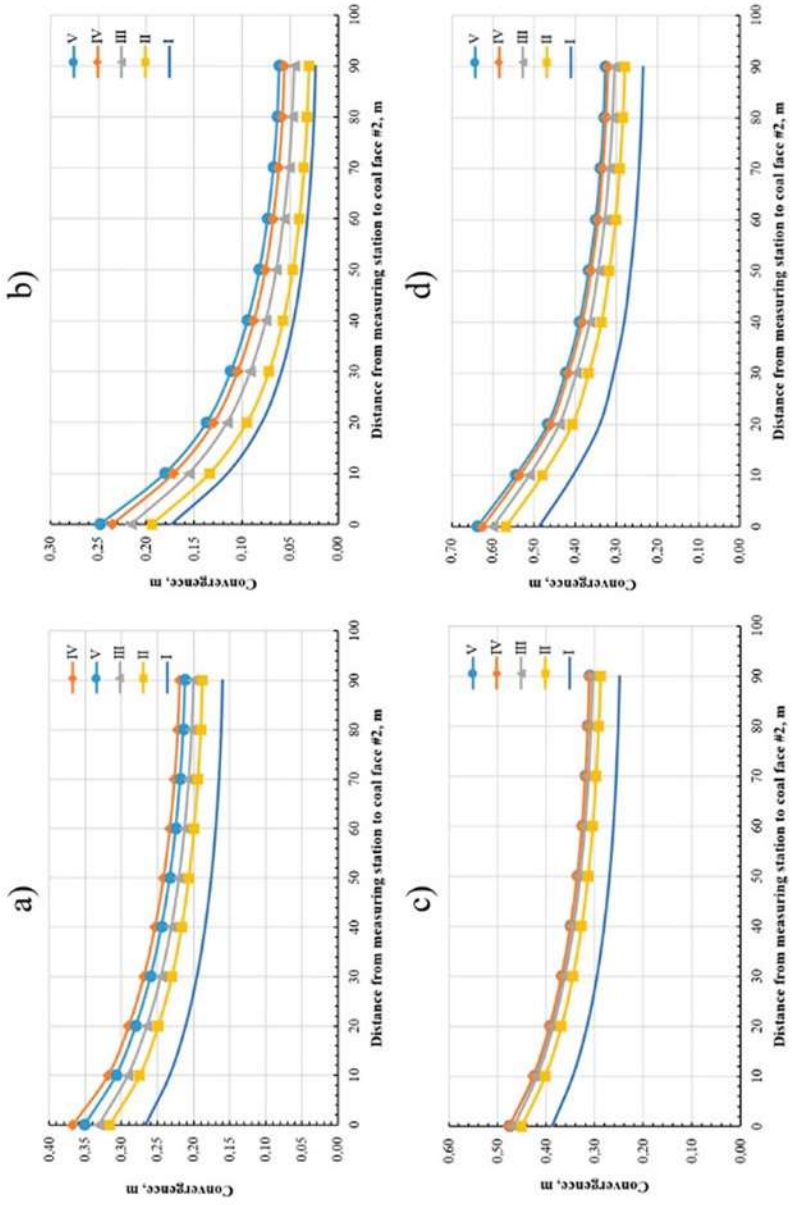

Fig. 8 Convergence of roadway before the coal face #2 corresponding to different roof rock structures: **a** roof subsidence, **b** convergence of the left rib (coal seam side), **c** convergence of the right rib (coal pillar side), **d** heaving of the floor